
REMOTE SENSING OF BIOMASS

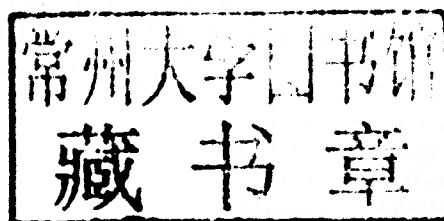
PRINCIPLES AND APPLICATIONS

Edited by **Temilola Fatoyinbo**



REMOTE SENSING OF BIOMASS – PRINCIPLES AND APPLICATIONS

Edited by Temilola Fatoyinbo



INTECHOPEN.COM

Remote Sensing of Biomass – Principles and Applications

Edited by Temilola Fatoyinbo

Published by InTech

Janeza Trdine 9, 51000 Rijeka, Croatia

Copyright © 2012 InTech

All chapters are Open Access distributed under the Creative Commons Attribution 3.0 license, which allows users to download, copy and build upon published articles even for commercial purposes, as long as the author and publisher are properly credited, which ensures maximum dissemination and a wider impact of our publications. After this work has been published by InTech, authors have the right to republish it, in whole or part, in any publication of which they are the author, and to make other personal use of the work. Any republication, referencing or personal use of the work must explicitly identify the original source.

As for readers, this license allows users to download, copy and build upon published chapters even for commercial purposes, as long as the author and publisher are properly credited, which ensures maximum dissemination and a wider impact of our publications.

Notice

Statements and opinions expressed in the chapters are these of the individual contributors and not necessarily those of the editors or publisher. No responsibility is accepted for the accuracy of information contained in the published chapters. The publisher assumes no responsibility for any damage or injury to persons or property arising out of the use of any materials, instructions, methods or ideas contained in the book.

Publishing Process Manager Niksa Mandić

Technical Editor Teodora Smiljanic

Cover Designer InTech Design Team

First published March, 2012

Printed in Croatia

A free online edition of this book is available at www.intechopen.com

Additional hard copies can be obtained from orders@intechopen.com

Remote Sensing of Biomass – Principles and Applications, Edited by Temilola Fatoyinbo
p. cm.

ISBN 978-953-51-0313-4

INTECH

open science | open minds

free online editions of InTech
Books and Journals can be found at
www.intechopen.com

Preface

The accurate measurement of ecosystem biomass is of great importance in scientific, resource management and energy sectors. In particular, biomass is a direct measurement of carbon storage within an ecosystem and of great importance for carbon cycle science and carbon emission mitigation. Closing the global carbon budget is one of the greatest scientific and societal needs of our time. Quantifying the carbon cycle is the most important element in understanding climate change and its consequences, yet is poorly understood (Le Toan et al, 2004). As an example, globally forests store 85% of terrestrial carbon, yet the amount of carbon contained in the earth's forests is not known to even one significant figure, ranging from 385 to 650 10^{15} g carbon (Saugier et al. 2001, Goodale et al. 2002, Houghton et al. 2009). It is therefore crucial that biomass measurements be improved.

Measurements of ecosystem biomass have far ranging societal, policy and management implications. The anticipated economic and societal burden that will result from unmitigated rises in CO₂ emissions and losses in ecosystem services alone are estimated to be in the trillion of dollars by mid-century (Stern Report, 2008). Ongoing international carbon mitigation initiatives need detailed, precise and accurate measurements of carbon storage in terrestrial, coastal and aquatic ecosystems to be successful.

Remote Sensing is the most accurate tool for global biomass measurements because of the ability to measure large areas. Current biomass estimates are derived primarily from ground-based samples, as compiled and reported in inventories and ecosystem samples. By using remote sensing technologies, we are able to scale up the sample values and supply wall to wall mapping of biomass. Three separate remote sensing technologies are available today to measure ecosystem biomass: passive optical, radar, and lidar.

There are many measurement methodologies that range from the application driven to the most technologically cutting-edge. The goal of this book is to address the newest developments in biomass measurements, sensor development, field measurements and modeling. The chapters in this book are separated into five main sections.

In section I (Forests) the authors present recent developments in remote sensing using lidar in Chapter 1 *Lidar Remote Sensing for Biomass Assessment* by J. Rosette, et al., Synthetic Aperture Radar in Chapter 2 *Forest Structure Retrieval from Multi-Baseline SAR tomography*, by S. Tebaldini, and very high resolution optical imagery in Chapter 3 *Biomass Prediction in Tropical Forest: the Canopy Grain Approach* by C. Proisy et al. In Chapter 4 *Remote Sensing of Biomass in the Miombo Woodlands of Southern Africa: opportunities and limitations for research*, N. Ribeiro et al lead us through a review of the current state of biomass estimation in Woodland forests of Southern Africa.

Section II (Oceans) of this book addresses biomass estimation of biomass in the oceans. In chapter 5 *Remote Sensing of Marine Phytoplankton Biomass*, T. Moisan et al. provide a review of the remote sensing techniques currently used in phytoplankton biomass estimation from space. In Chapter 6 *Using SVD analysis of combined altimetry and ocean color satellite data for assessing basin scale physical-biological coupling in the Mediterranean Sea*, the authors A. Jordi and G. Basterretxea analyze patterns of phytoplankton variability at inter-annual, seasonal and intra-annual scales in the Mediterranean Sea based on satellite imagery.

Section III (Fires) addresses the remote sensing of fires and post-fire monitoring in forests. In Chapter 7 *Advances in Remote Sensing of Post-Fire Monitoring*, I. Gitas et al. carry out a detailed review of the current state of remote sensing of burned forest areas. Chapter 8 *The science and application of Satellite Based Fire radiative energy* by E. Elicott and E. Vermote examines the effect of forest biomass burning on the biosphere and atmosphere.

In Section IV (Models), the chapters address the combination of remote sensing and ecosystem modeling as they relate to biomass. Chapter 9. *Resilience and stability associated with conversion of boreal forest* by J.K. Shuman and H.H. Shugart examines the forest composition and biomass across Siberia and the Russian Far East from individual based modeling and remote sensing to evaluate forest response to climate change. In chapter 10 *Estimating biomass dynamics from LAI through a plant model*, M. Kang et al present a model of plant growth from noisy and incomplete remote sensing data.

Section V (Applications) composed of chapters where biomass is estimated for resource management or agricultural applications. In Chapter 11 *Mapping aboveground and foliage biomass over the Porcupine caribou habitat in northern Yukon and Alaska using Landsat and JERS-1/SAR data*, W. Chen et al. develop baseline maps of aboveground and foliage biomass of forested and non forested areas over the Porcupine caribou habitat in northern Yukon and Alaska, using Landsat and JERS-1/SAR data. Chapter 12 *Rice Crop Monitoring with Unmanned Helicopter Remote Sensing Images* by K. Swain et al. explores the use of unmanned Helicopter Remote sensing for precision agriculture and biomass yield estimations in rice plantations. In Chapter 13 *Geostatistical Estimation of Biomass Stock in Chilean Native Forests and Plantations*, the authors J.

Hernandez et al. create and validate methods for the estimation of above ground biomass in Chile using medium spatial resolution satellite imagery, digital elevation models and geostatistical modeling. Finally, Chapter 14 *Using Remote Sensing To Estimate A Renewable Resource: Forest Residual Biomass* by A. García-Martín et al. describes a methodology developed to estimate the amount of Forest Residual Biomass potentially suitable for renewable energy production in the pine forests of Mediterranean areas at regional scales, using optical satellite images and forest inventory data.

Temilola Fatoyinbo

Biospheric Sciences Laboratory, NASA Goddard Space Flight Center, Greenbelt, MD,
USA

Contents

Preface IX

Part 1 Forests 1

- Chapter 1 **Lidar Remote Sensing for Biomass Assessment 3**
Jacqueline Rosette, Juan Suárez,
Ross Nelson, Sietse Los,
Bruce Cook and Peter North
- Chapter 2 **Forest Structure Retrieval from
Multi-Baseline SARs 27**
Stefano Tebaldini
- Chapter 3 **Biomass Prediction in Tropical Forests:
The Canopy Grain Approach 59**
Christophe Proisy, Nicolas Barbier,
Michael Guérault, Raphael Pélissier,
Jean-Philippe Gastellu-Etchegorry,
Eloi Grau and Pierre Couteron
- Chapter 4 **Remote Sensing of Biomass in
the Miombo Woodlands of Southern Africa:
Opportunities and Limitations for Research 77**
Natasha Ribeiro, Micas Cumbana,
Faruk Mamugy and Aniceto Chaúque
- Part 2 Oceans 99**
- Chapter 5 **Ocean Color Remote Sensing of
Phytoplankton Functional Types 101**
Tiffany A.H. Moisan,
Shubha Sathyendranath and Heather A. Bouman
- Chapter 6 **Using SVD Analysis of Combined Altimetry and
Ocean Color Satellite Data for Assessing Basin Scale
Physical-Biological Coupling in the Mediterranean Sea 123**
Antoni Jordi and Gotzon Basterretxea

Part 3 Fires 141

- Chapter 7 **Advances in Remote Sensing of Post-Fire Vegetation Recovery Monitoring – A Review 143**

Ioannis Gitas, George Mitri,
Sander Veraverbeke and Anastasia Polychronaki

- Chapter 8 **The Science and Application of Satellite Based Fire Radiative Energy 177**

Evan Ellicott and Eric Vermote

Part 4 Models 193

- Chapter 9 **Resilience and Stability Associated with Conversion of Boreal Forest 195**

Jacquelyn Krempfer Shuman and Herman Henry Shugart

- Chapter 10 **Reconstructing LAI Series by Filtering Technique and a Dynamic Plant Model 217**

Meng Zhen Kang, Thomas Corpetti,
Jing Hua and Philippe de Reffye

Part 5 Applications 229

- Chapter 11 **Mapping Aboveground and Foliage Biomass Over the Porcupine Caribou Habitat in Northern Yukon and Alaska Using Landsat and JERS-1/SAR Data 231**

Wenjun Chen, Weirong Chen, Junhua Li, Yu Zhang,
Robert Fraser, Ian Olthof, Sylvain G. Leblanc and Zhaohua Chen

- Chapter 12 **Rice Crop Monitoring with Unmanned Helicopter Remote Sensing Images 253**

Kishore C. Swain and Qamar Uz Zaman

- Chapter 13 **Geostatistical Estimation of Biomass Stock in Chilean Native Forests and Plantations 273**

Jaime Hernández, Patricio Corvalán,
Xavier Emery, Karen Peña and Sergio Donoso

- Chapter 14 **Using Remote Sensing to Estimate a Renewable Resource: Forest Residual Biomass 297**

A. García-Martín, J. de la Riva, F. Pérez-Cabello and R. Montorio

Part 1

Forests

Lidar Remote Sensing for Biomass Assessment

Jacqueline Rosette^{1,3,4}, Juan Suárez^{2,4}, Ross Nelson³,
Sietse Los¹, Bruce Cook³ and Peter North¹

¹*Swansea University,*

²*Forest Research*

³*NASA Goddard Space Flight Center,*

⁴*University of Maryland College Park*

^{1,2}*United Kingdom*

^{3,4}*USA*

1. Introduction

Optical remote sensing provides us with a two dimensional representation of land-surface vegetation and its reflectance properties which can be indirectly related to biophysical parameters (e.g. NDVI, LAI, fAPAR, and vegetation cover fraction). However, in our interpretation of the world around us, we use a three-dimensional perspective. The addition of a vertical dimension allows us to gain information to help understand and interpret our surroundings by considering features in the context of their size, volume and spatial relation to each other.

In contrast to estimates of vegetation parameters which can be obtained from passive optical data, active lidar remote sensing offers a unique means of directly estimating biophysical parameters using physical interactions of the emitted laser pulse with the vegetation structure being illuminated. This enables the vertical profile of the vegetation canopy to be represented, not only permitting canopy height, metrics and cover to be calculated but also enabling these to be related to other biophysical parameters such as biomass.

This chapter provides an overview of this technology, giving examples of how lidar data have been applied for forest biomass assessment at different scales from the perspective of satellite, airborne and terrestrial platforms. The chapter concludes with a discussion of further applications of lidar data and a look to the future towards emerging lidar developments.

1.1 Context

Aside from destructive sampling, traditional methods of calculating biomass for forest inventory, monitoring and management often rely on taking field measurements within sample plots, such as diameter at breast height (DBH) or Top/Lorey's height. This effort can be time, cost and labour intensive. Extrapolation of field measurements to larger areas relies on representative sampling of trees within a land-cover type and correct classification of land cover over large areas; both of which have inherent uncertainties.

Lidar remote sensing complements traditional field methods through data analysis which enables the extraction of vegetation parameters that are commonly measured in the field.

Additionally, establishing allometric relationships between lidar and field measurements enables estimates to be extrapolated to stand, forest or national scales, which would not be feasible or very costly using field survey methods alone. Key aspects of biomass estimation from satellite, airborne and terrestrial lidar systems are outlined below.

1.2 Principles of lidar remote sensing

When walking through a woodland on a sunny day, some of the sunlight reaches the ground through gaps between the foliage, woody branches and stems; some produces more diffuse light at the ground by transmittance through the foliage or reflection between different vegetation components and the ground, and some is absorbed by the intercepted surfaces. A proportion of the energy is reflected from these surfaces back towards the source. The same principles apply to lidar.

Lidar (Light Detection and Ranging) is an active remote sensing technology, which involves the emission of laser pulses from the instrument positioned on a platform, towards a target (e.g. woodland). Here, it interacts with the different surfaces it intercepts as outlined above (Figure 1). Features further from the sensor will intercept and reflect the laser energy back to the sensor later than those closer to it.

The area which is illuminated by the laser pulse is known as the lidar 'footprint'. The size of the footprint is determined by the laser divergence and the altitude/distance from the target of the lidar instrument. Whether the footprint is of large dimensions in the region of tens of metres from the altitude of a satellite sensor, tens of centimetres as generally produced from airborne platforms or several millimetres in the case of terrestrial laser scanners, the principles remain the same.

Interactions of the laser pulse with the vegetation depend on the wavelength of the emitted pulse and its reflectance, transmittance and absorption rates for each foliage, bark and background type (e.g. bare soil, litter, snow, etc). At wavelengths of 1064 nm (in the near-infrared region of the spectrum and typical of many lidar systems used for vegetation analysis), reflectance and transmittance values may each be commonly ~45%.

The time for the reflected pulse echoes to be returned to the sensor is measured and, using the fact that the laser pulse travels at the speed of light, the total return distance travelled between the sensor and the intercepted surfaces can be calculated. The distance between the altimeter and the intercepted object is therefore half of this value (Baltsavias, 1999; Wehr *et al.*, 1999). This permits the three-dimensional reproduction of the Earth surface relief and above-surface object structures (e.g. vegetation, ice cover, atmospheric aerosols and cloud structure).

Very accurate timing is necessary to obtain fine vertical resolutions. Lidar time units are generally recorded in nanoseconds (ns), each being equal to approximately 15cm in one-way distance between the sensor and target. Time is measured by a time interval counter, initiated on emission of the pulse and triggered at a specific point on the leading edge of the returned pulse. This position is not immediately evident and therefore is set to occur where the signal voltage reaches a pre-determined threshold value. The steepness of the received pulse (rise time of the pulse) is a principal contributory factor to range accuracy and depends on the combination of numerous factors such as incident light wavelength, reflectivity of targets at that wavelength, spatial distribution of laser energy across the footprint and atmospheric attenuation (Baltsavias, 1999). The return pulse leading edge rise time is therefore formed by the strength of the return signal from the highest intercepted

surfaces within the footprint. This will vary with the nature of the surface; flat ice sheets producing abrupt returns with fast leading edge rises and multilayered, complex vegetation creating broad returns (Harding *et al.*, 1998; Ni-Meister *et al.*, 2001).

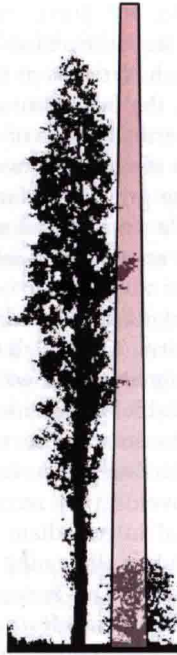


Fig. 1. Representation of the interception of foliage, bark or ground surfaces by an emitted laser pulse. At each surface, some energy is reflected, transmitted (in the case of foliage) or absorbed.

The location of every returned signal to a known coordinate system is achieved by precise kinematic positioning using differential GPS and orientation parameters by the Inertial Measurement Unit (IMU). The IMU captures orientation parameters of the instrument platform such as pitch, roll and yaw angles. Therefore, the GPS provides the coordinates of the laser source and the IMU indicates the direction of the pulse. With the ranging data accurately measured and time-tagged by the clock, the position of the returned signal can be calculated.

1.3 Full waveform and discrete return systems

A waveform is the signal that is returned to the lidar sensor after having been scattered from surfaces that the laser pulse intercepts. Full waveform lidar systems record the entire returned signal within an elevation range window above a background energy noise threshold. An example of this from NASA's Geoscience Laser Altimeter System (GLAS; Section 2) is shown in Figure 2 (left). The scene shows a two-storey Douglas Fir canopy (*Pseudotsuga menziesii*) on a gentle slope of 4.9°. Typically, for vegetated surfaces on relatively flat ground, a bimodal waveform is produced.

The beginning and end of the waveform signal above the background noise threshold are represented by the upper and lower horizontal blue lines respectively (mean noise + 4.5σ in the case of GLAS). Amplitude of the waveform (x axis) represents both intercepted surface area at each elevation plus the reflectivity of the surfaces at the emitted wavelength (1064nm).

The gradient at the beginning of the signal increases slowly initially due to the relatively small surface area of foliage and branch elements at the uppermost canopy. As the energy penetrates down through the canopy, the waveform amplitude increases as more features are intercepted, before decreasing towards the base of the tree crowns. A small peak, which corresponds to a shorter tree, can be observed above the abrupt, narrow peak, which is returned from the ground. Below the ground surface, the signal can be seen to trail off gradually. This relates to both a gentle slope found at this site plus the effect of multiple scattering between features within the scene, which serves to delay part of the signal that is returned to the sensor.

Due to the complex waveform signal which is produced, this is often simplified using Gaussian decomposition of the waveform (Figure 2, left). Representing the waveform as the sum of the Gaussians, smoothes the signal yet allows a means of retaining and identifying the dominant characteristics of the signal for easier interpretation.

Small footprint lidar systems can produce dense sampling of the target surface. The returned signal is also in the form of a waveform, however with discrete return systems, only designated echoes within the waveform are recorded. These can be the first and last returns, or at times, also a number of intermediate points. The amalgamation of these returns from multiple emitted lidar pulses allows the scene to be reconstructed as a 'point cloud' of geolocated intercepted surfaces. This is seen in Figure 2, right, which illustrates the same location as seen within the GLAS waveform. The small footprint lidar point cloud can be interpreted more intuitively as a dominant upper storey of approximately uniform height and a single tree of lower height at the centre of the scene. Points are coloured with respect to their elevation.

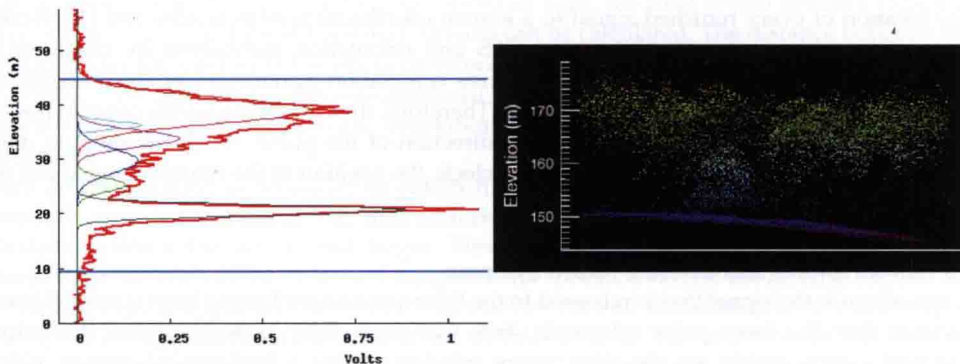


Fig. 2. Example of a waveform produced by a large footprint lidar system (left) and a discrete return lidar point cloud (right) for a coincident area. Location: Forest of Dean, Gloucestershire, UK

1.4 Lidar footprint distribution patterns

Distribution patterns of footprints differ between lidar systems. Lidar profiling involves the systematic location of footprints at intervals along the sensor's path on the ground. These may be contiguous such as the Portable Airborne Laser System of Nelson *et al.*, 2003 (PALS), or placed at discontinuous distances along the ground track in the case of NASA's Geoscience Laser Altimeter System, GLAS (Schutz *et al.*, 2005). This generally permits the sampling of extensive areas, however requires a means to extrapolate biophysical parameter estimates for areas where data were not acquired.

Laser scanning, obtained from an airborne platform, occurs perpendicular to the direction of travel and generally produces a dense distribution of small footprints. Swath width and footprint density are dependent on the altitude and speed of the aircraft plus the scan angle applied. A scanning mirror directs laser pulses back and forth across the flightline causing data to be captured typically in a sawtooth arrangement. The maximum off-nadir scan angle for the instrument can be customised according to the needs of each campaign. Narrower scan angles improve the chances of each shot penetrating dense vegetation canopies and of the sensor receiving a returned pulse from the ground as there is greater likelihood of a clear path through the canopy to the ground. The usual practice is to create an overlap of flightlines similar to photogrammetric surveys of ~60%. Multiple flightlines can then be combined to provide full coverage of the desired area by means of specialised software. Small footprint laser scanning is generally operated at the forest scale, largely due to cost implications.

1.5 Lidar system configurations

As discussed above, lidar sensors can be operated at different scales from different altitudes and different viewing perspectives in relation to the target surface; from above in the case of satellite and airborne systems and from below or to the side for terrestrial laser scanners. Lidar instrument specifications therefore vary considerably, combining different sampling patterns on the ground, density and size of individual laser footprints.

Nelson *et al.*'s (2008; 2003; 2004) PALS is an example of a small footprint, discrete return, lidar profiler which is operated from an aircraft. Its innovative and portable design has permitted sampling and vegetation parameter estimation at regional scales throughout the world and may be considered a predecessor to the satellite lidar profiling sensor discussed in Section 2.

The Laser Vegetation Imaging Sensor (LVIS) is an experimental lidar instrument developed at NASA Goddard Space Flight Center (GSFC, 2010). It is a full waveform, scanning lidar that emits a 1064 nm laser beam at a pulse repetition rate of 100-500Hz. LVIS can operate at an altitude in excess of 10 km and this offers the capability of producing swaths up to two km wide and medium-sized footprints of 1-80 m diameter (Blair *et al.*, 1999; Dubayah *et al.*, 2010; GSFC, 2010).

Until relatively recently, small footprint lidar were almost exclusively restricted to discrete return systems within the commercial and operational sector whilst full waveform instruments remained a research and development tool. It should be noted that recent advances in data storage capacity are beginning to open opportunities for small footprint, full waveform scanning systems, however to date, software to process such data is not readily available.

By necessity, this chapter cannot attempt to fully present all combinations of lidar specifications. Readers should note that the multiple vegetation applications of lidar data lead

to wide-ranging variations in sensor design and characteristics as outlined above. In the descriptions within sections 2-4, an example of a satellite sensor is used to demonstrate the principles of large footprint, full waveform profiling data, whilst airborne and terrestrial lidar instruments are used to provide examples of small footprint, discrete return laser scanning.

1.6 Key concepts for biomass assessment

Lidar remote sensing provides a direct estimation of the elevation of intercepted features. In the context of vegetation, if signals from the ground and vegetation can be distinguished, the relative heights above ground of forest canopies can be calculated. Since an adequate stem diameter and canopy structure are needed to support tree dimensions, vegetation height is closely related to volume and therefore biomass. The sections below provide examples of applications of lidar systems for biomass assessment.

2. Satellite lidar profiling

NASA's Geoscience Laser Altimeter System (GLAS) aboard the Ice, Cloud and land Elevation Satellite (ICESat) is currently the only satellite lidar system to have provided near global sampling coverage over an extended period of time. It therefore offers a unique dataset of vertical profiles of the Earth's surface.

ICESat was launched in January 2003 and the mission continued until the final laser ceased firing in the Autumn of 2009. During this period, the laser was operated for approximately month-long periods annually during Spring and Autumn, and additionally during the Summer earlier in the mission lifetime.

This is a full waveform, lidar profiling system which operated at an altitude of 600km, travelling at 26,000 km h⁻¹ and emitting 1064nm laser pulses at 40Hz. This caused the Earth's surface to be sampled at intervals with footprint centres positioned 172m apart. Footprint diameter and eccentricity have varied considerably between laser campaigns from a major axis of 148.6±9.8m to 51.2±1.7m (Figure 3). Comprehensive information regarding the sensor are available from Abshire *et al.*, 2005; Brenner *et al.*, 2003; NSIDC, 2010a; Schutz *et al.*, 2005; Schutz, 2002. Data plus tools to process them are available free of charge from NSIDC, 2010b.

2.1 Characteristics

The systematic sampling pattern and representation of the vegetation profile within the returned lidar waveform signal (Figure 2, left) enables the spatial distribution of vegetation parameters to be mapped for large areas. The seasonal coverage allows near repeat measurements at a frequency which would not be feasible using conventional survey methods. However the system was designed primarily for cryospheric applications and therefore the configuration is not considered optimal for vegetation analysis. This poses some challenges for forestry applications. Upon sloped, vegetated terrain, vegetation and ground surfaces may occur at the same elevations. This causes the signals from ground and vegetation to be combined within the waveform and, where it is not possible to distinguish a ground peak, this prevents the signal returned from the vegetation from being reasonably identified. Furthermore, dense cloud cover prevents a valid return signal causing gaps in footprint sampling (Figure 3). For regions with high cloud cover such as the tropics, this can serve to worsen the already-sparse sampling density near the equator, produced by the polar orbit.